

Theory of mirror benchmarking and demonstration on a quantum computer

Karl Mayer, Alex Hall, Thomas Gatterman, Si Khadir Halit, Kenny Lee, Justin Bohnet, Dan Gresh, Aaron Hankin, Kevin Gilmore, Justin Gerber, and John Gaebler
Honeywell Quantum Solutions
 (Dated: June 5, 2023)

A new class of protocols called mirror benchmarking was recently proposed to measure the system-level performance of quantum computers. These protocols involve circuits with random sequences of gates followed by mirroring, that is, inverting each gate in the sequence. We give a simple proof that mirror benchmarking leads to an exponential decay of the survival probability with sequence length, under the uniform noise assumption, provided the twirling group forms a 2-design. The decay rate is determined by a quantity that is a quadratic function of the error channel, and for certain types of errors is equal to the unitarity. This result yields a new method for estimating the coherence of noise. We present data from mirror benchmarking experiments run on the Honeywell System Model H1. This data constitutes a set of performance curves, indicating the success probability for random circuits as a function of qubit number and circuit depth.

I. INTRODUCTION

Quantum computers are expected to someday solve problems that are intractable for classical computers, but what are the capabilities of quantum computers today? How should the performance of quantum computers be measured? Perhaps surprisingly, there is no agreed upon answer to these questions, though a number of metrics have been proposed. One such metric, the quantum volume (QV), is given by the maximum number of qubits for which a class of random circuits produces a distribution that passes a certain statistical test [1]. Other groups have proposed to use textbook algorithms such as Bernstein-Vazirani or Grover search, which ideally produce deterministic outputs, and report the algorithmic success probability [2]. Other proposals, inspired by randomized benchmarking (RB) [3, 4], employ random Clifford circuits of varying length, which can be inverted in order to measure the survival probability [5]. There are advantages and disadvantages to each of these system-level benchmarks, which have been discussed elsewhere [6].

In this paper, we focus on a protocol referred to as mirror benchmarking, of which different versions were proposed in [7]. In the variation we consider, the first half of a circuit consists of a sequence of randomly chosen layers, and the second half applies the inverse of each layer in reverse order, so that the final state is ideally equal to the initial state. Additionally, random Pauli gates can be inserted between layers to remove coherent effects, similar to the randomized compiling procedure [8]. The output of mirror benchmarking is a plot of the survival probability as a function of the sequence length. This can be useful to a quantum computer user as it provides a direct measure of circuit performance for a given qubit number and circuit depth.

The authors of [7] provide substantial motivation for why mirror benchmarking is a useful benchmark. They also advocate for the use of mirroring broadly, to benchmark any circuit of interest, rather than just random circuits as described here. Restricting our attention to

random circuits, our main contribution is a formula for how the survival probability decays as a function of sequence length, in analogy to RB protocols. We show that under assumptions commonly made in RB research, the survival probability decays exponentially. Under some additional assumptions on the noise, the decay parameter is the unitarity of the average error per circuit layer. The unitarity was introduced in [9] and is a measure of the coherence of noise. A consequence of this result is that besides being a useful benchmark for system-level performance, mirror benchmarking provides a new method to estimate the unitarity of noise, for instance of a two-qubit gate. This requires fewer circuits than the protocol of [9].

We implement mirror benchmarking on the Honeywell System Model H1 quantum computer. In our implementation, each layer consists of a random single-qubit Clifford gate on each qubit, followed by a native two-qubit gate applied to each qubit pair in a random fully-connected pairing of qubits. We run mirror benchmarking on $n = 6, 8, 10$ qubits. For the largest circuits run in this experiment, with $n = 10$ and sequence length $L = 16$, corresponding to a two-qubit circuit depth of 32 and 160 total two-qubit gates, we obtain an average survival probability of 0.344(18).

The outline of this paper is as follows. In Sec. II we give a simple proof that the survival probability in mirror benchmarking decays with a rate determined by the unitarity. In Sec. III we address the question of how accurately the direct sampling of gates used in our experiment approximates a true uniform sampling over a 2-design. In Sec. IV we describe our implementation of mirror benchmarking on the Honeywell System Model H1 quantum computer and present the results. Finally, Sec. V contains a discussion and conclusion.

II. MIRROR BENCHMARKING SURVIVAL PROBABILITY

In a mirror benchmarking protocol, a sequence of unitaries g_1, \dots, g_L , followed by their inverses $g_L^{-1}, \dots, g_1^{-1}$, is applied to a noisy initial state, given by density matrix ρ . For the present discussion, the g_i may be individual gates, or more complicated sequences of gates, but we assume that they are sampled uniformly at random from a group G that forms a unitary 2-design [10]. Let \mathcal{E} be a constant error channel associated with each unitary in the sequence. We assume that \mathcal{E} is unital, that is, $\mathcal{E}(I) = I$, but we discuss how to relax this assumption in the appendix. We also assume that the error channel per unitary during the inversion half of the circuit is given by \mathcal{E}^\dagger , the dual of \mathcal{E} , which is defined by $\langle\langle \mathcal{E}^\dagger(M)|N \rangle\rangle = \langle\langle M|\mathcal{E}(N) \rangle\rangle$, where $\langle\langle M|N \rangle\rangle := \text{Tr}(M^\dagger N)$. We postpone a discussion of this assumption to the end of this section.

At the end of the circuit a measurement is performed that is described by a noisy POVM with elements $\{E, I - E\}$. The average survival probability for a sequence of length L is then given by

$$p(L) = \frac{1}{|G|^L} \sum_{g_1, \dots, g_L} \langle\langle E | \mathcal{E}^\dagger g_1^{-1} \dots \mathcal{E}^\dagger g_L^{-1} \mathcal{E} g_L \dots \mathcal{E} g_1 | \rho \rangle\rangle, \quad (1)$$

where by abuse of notation we use g to denote both a unitary and its corresponding superoperator. We can absorb the final \mathcal{E}^\dagger into the noisy POVM element E , and after defining $g_{i'} = g_i \dots g_{2L} g_1$ and relabeling $g_{i'} \mapsto g_i$, the survival probability can be written as

$$p(L) = \frac{1}{|G|^L} \sum_{g_1, \dots, g_L \in G} \langle\langle E | (g_1^{-1} \mathcal{E}^\dagger g_1) \dots (g_L^{-1} \mathcal{E}^\dagger g_L) (g_L \mathcal{E} g_L) \dots (g_1 \mathcal{E} g_1) | \rho \rangle\rangle. \quad (2)$$

An important quantity is the twirl of \mathcal{E} over G , which is defined as

$$\mathcal{E}_T = \frac{1}{|G|} \sum_{g \in G} g^{-1} \mathcal{E} g. \quad (3)$$

A useful fact is that \mathcal{E}_T commutes with g for all $g \in G$, which can be shown as follows:

$$\begin{aligned} g \mathcal{E}_T &= \frac{1}{|G|} \sum_{h \in G} g h^{-1} \mathcal{E} h \\ &= \frac{1}{|G|} \sum_{h \in G} (h g^{-1})^{-1} \mathcal{E} (h g^{-1}) g \\ &= \frac{1}{|G|} \sum_{h' \in G} (h')^{-1} \mathcal{E} h' g \\ &= \mathcal{E}_T g, \end{aligned} \quad (4)$$

where in the third line we set $h' = h g^{-1}$, and used the group transitivity property to change the index of summation from h to h' .

Summing over g_L in Eq. (2), and using Eq. (4), the central terms in the product in Eq. (2) are then

$$(g_{L-1}^{-1} \mathcal{E}^\dagger g_{L-1}) \mathcal{E}_T (g_{L-1}^{-1} \mathcal{E} g_{L-1}) = g_{L-1}^{-1} \mathcal{E}^\dagger \mathcal{E}_T \mathcal{E} g_{L-1}. \quad (5)$$

Summing the right hand side of Eq. (5) over g_{L-1} ,

$$\frac{1}{|G|} \sum_{g_{L-1}} g_{L-1}^{-1} \mathcal{E}^\dagger \mathcal{E}_T \mathcal{E} g_{L-1} = (\mathcal{E}^\dagger \mathcal{E}_T \mathcal{E})_T. \quad (6)$$

Continuing in this way, the general pattern for the survival probability at sequence length L can be described recursively as follows. Let \mathcal{T}_l for $l = 1, 2, \dots$ be the sequence of operators defined by $\mathcal{T}_1 = \mathcal{E}_T$ and $\mathcal{T}_{l+1} = (\mathcal{E}^\dagger \mathcal{T}_l \mathcal{E})_T$. Then

$$p(L) = \langle\langle E | \mathcal{T}_L | \rho \rangle\rangle. \quad (7)$$

We will derive an expression for \mathcal{T}_L . First we recall some facts about twirls over 2-designs [10]. Let $\mathcal{B}(\mathcal{H})$ denote the vector space of linear operators on Hilbert space $\mathcal{H} = \mathbb{C}^d$. Let $V_1 = \text{span}\{I\}$ and $V_2 = \{A \in \mathcal{B}(\mathcal{H}) : \text{Tr}(A) = 0\}$, and note that $\mathcal{B}(\mathcal{H}) = V_1 \oplus V_2$. Let $\mathcal{M} : \mathcal{B}(\mathcal{H}) \rightarrow \mathcal{B}(\mathcal{H})$ and suppose that G is a 2-design. Then the twirl of \mathcal{M} over G is a linear combination of two projectors:

$$\mathcal{M}_T = a \Pi_1 + b \Pi_2, \quad (8)$$

where Π_1 and Π_2 are the projectors onto V_1 and V_2 , respectively (A proof of this fact that does not rely on representation theory is found in [11]). If \mathcal{M} is trace-preserving (TP), then \mathcal{M}_T is also TP, and therefore

$$\text{Tr}(I) = \text{Tr}(\mathcal{M}_T(I)) = a \text{Tr}(\Pi_1 I) = a \text{Tr}(I), \quad (9)$$

which implies that $a = 1$. Let $D = \dim(V_2) = d^2 - 1$. The quantity b is given by

$$\begin{aligned} b &= \frac{1}{D} \text{Tr}(\Pi_2 \mathcal{M}_T) \\ &= \frac{1}{D} \frac{1}{|G|} \sum_{g \in G} \text{Tr}(g \Pi_2 g^{-1} \mathcal{M}) \\ &= \frac{1}{D} \text{Tr}(\Pi_2 \mathcal{M}), \end{aligned} \quad (10)$$

where in the last equality we used the fact that Π_2 commutes with the action of G . Given an error channel \mathcal{E} , define

$$f(\mathcal{E}) = \frac{1}{D} \text{Tr}(\Pi_2 \mathcal{E}). \quad (11)$$

The quantity $f(\mathcal{E})$ is related to $F(\mathcal{E})$, the process fidelity (also called entanglement fidelity) with respect to the identity [11], according to

$$1 - f(\mathcal{E}) = \frac{d^2}{D} (1 - F(\mathcal{E})). \quad (12)$$

We will simply write f when the channel \mathcal{E} is clear from context. By Eqs. (7)-(10), we have

$$\mathcal{E}_T = \Pi_1 + f\Pi_2. \quad (13)$$

The unitarity of \mathcal{E} , which was introduced in [9], is given by

$$u = \frac{1}{D} \text{Tr}(\Pi_2 \mathcal{E}^\dagger \Pi_2 \mathcal{E}). \quad (14)$$

We are now ready to prove a formula for the survival probability.

Lemma 1. *Let \mathcal{T}_l for $l = 1, 2, \dots$ be a sequence of operators defined by $\mathcal{T}_1 = \mathcal{E}_T$, and $\mathcal{T}_{l+1} = (\mathcal{E}^\dagger \mathcal{T}_l \mathcal{E})_T$. Then for all l ,*

$$\mathcal{T}_l = \Pi_1 + fu^{l-1}\Pi_2.$$

Proof. We proceed by induction. The base case is given by Eq. (13). Suppose the statement is true for a particular l . Then

$$\begin{aligned} \mathcal{T}_{l+1} &= (\mathcal{E}^\dagger (\Pi_1 + fu^{l-1}\Pi_2) \mathcal{E})_T \\ &= \Pi_1 + \frac{1}{D} \text{Tr}(\Pi_2 (\mathcal{E}^\dagger (\Pi_1 + fu^{l-1}\Pi_2) \mathcal{E})) \Pi_2, \end{aligned} \quad (15)$$

where in the second equality we used Eqs. (8) and (10) with $\mathcal{M} = \mathcal{E}^\dagger (\Pi_1 + fu^{l-1}\Pi_2) \mathcal{E}$. Since \mathcal{E} is trace preserving, $\Pi_1 \mathcal{E} \Pi_2 = 0$, from which it follows that

$$\text{Tr}(\Pi_2 \mathcal{E}^\dagger \Pi_1 \mathcal{E}) = \text{Tr}(\mathcal{E}^\dagger \Pi_1 \mathcal{E} \Pi_2) = 0. \quad (16)$$

Therefore,

$$\begin{aligned} \mathcal{T}_{l+1} &= \Pi_1 + \frac{1}{D} fu^{l-1} \text{Tr}(\Pi_2 \mathcal{E}^\dagger \Pi_2 \mathcal{E}) \Pi_2 \\ &= \Pi_1 + fu^l \Pi_2. \end{aligned} \quad (17)$$

□

Theorem 1. *The survival probability for mirror benchmarking is given by*

$$p(L) = Afu^{L-1} + B, \quad (18)$$

for constants A and B that depend only on the state prep and measurement.

Proof. This follows directly from Lemma 1 and Eq. (7) with $A = \langle\langle E | \Pi_2 | \rho \rangle\rangle$ and $B = \langle\langle E | \Pi_1 | \rho \rangle\rangle$. □

A few comments are in order. The assumption that the error channel during the inversion half of the circuit is \mathcal{E}^\dagger implies that a unitary error U on g_i will correspond to error U^{-1} on g_i^{-1} . This may not always hold but often can be enforced by a suitable compilation procedure. For example, if $g_i = e^{-iZZ\theta}$ is subject to a control error in θ , then g_i^{-1} may be implemented by $Pe^{-iZZ\theta}P$, for any Pauli P that anticommutes with ZZ . If we relax this assumption, and allow for an arbitrary error channel \mathcal{E}_{inv}

on the inverse gates, then the unitarity u in Th. 1 is replaced with $\frac{1}{D} \text{Tr}(\Pi_2 \mathcal{E}_{inv} \Pi_2 \mathcal{E})$.

In the limit of perfectly coherent errors, that is $u = 1$, the survival probability does not decay at all, since the coherent errors during the second half of the circuit under these assumptions exactly cancel those from the first half. At the other extreme, when the error is a depolarizing channel, $\mathcal{E} = \Pi_1 + f\Pi_2$ and therefore $u = f^2$ and $p(L) = Af^{2L-1} + B$. It is only in this special case that the decay parameter also extracts the fidelity of \mathcal{E} . If \mathcal{E} is a stochastic Pauli channel, which we assume in our experimental implementation by the use of Pauli randomization in the protocol, then $\mathcal{E} = \mathcal{E}^\dagger$ is diagonal in the Pauli basis of the superoperator representation. In this case, the unitarity is no longer a measure of coherent errors, but is still defined by Eq. (14). The process fidelity then is bounded in terms of the unitarity according to

$$\frac{1}{d^2} (1 + Du) \leq F(\mathcal{E}) \leq \frac{1}{d^2} (1 + D\sqrt{u}). \quad (19)$$

A derivation of this bound is given in the appendix.

III. DIRECT CIRCUIT SAMPLING

Theorem 1 of the previous section assumed that the group G is a 2-design. However, in the experiment described in the next section, each layer unitary g_i is sampled from a generating set for the n -qubit Clifford group C_n , rather than from the full group. This is done to avoid the need to compile a random Clifford group element, and so that the sequence lengths of the decay curve more directly correspond to two-qubit gate depth. Thus, our implementation of mirror benchmarking is analogous to the direct benchmarking protocol of [5]. Here, we justify the claim that Th. 1 should still approximately apply.

The problem of RB using a generating set for the Clifford group was studied in [12] as a Markov process on the Cayley graph of the Clifford group. The i -th element of the sequence, g_i , approximately samples from the group if an initial distribution over the generating set diffuses to an approximately uniform distribution over the full graph. We take a different approach, and simulate the distribution of unitaries $U^{(L)} = g_L \cdots g_2 g_1$ generated by sequences of length L , with the gate set used in our experiment and described in Sec. IV. A set of unitaries $\{U_i\}_i$ is a t -design if and only if

$$\Phi_t := \mathbb{E}_i |\text{Tr}(U_i)|^{2t} = t!, \quad (20)$$

where the quantity on the left hand side is called the t -th frame potential [13]. We numerically estimate the 2nd frame potential Φ_2 for the set $\{U_i^{(L)}\}_i$ generated by mirror benchmarking circuits of sequence length $L = 2, 4, \dots, 16$ and qubit numbers $n = 4, 6, 8$. The results are shown in Fig. 1. For each data point, we generated 10,000 random circuits and computed the quantity in Eq. (20), using the standard error for the error bars.

The plot shows convergence to the 2-design value, with faster convergence for smaller qubit number. For short sequence lengths, typically $L < n$, the gate set for direct mirror benchmarking circuits fails to approximate a 2-design, and therefore fitting $p(L)$ to a single exponential decay should be understood as a heuristic benchmark, rather than an unbiased estimate of the unitarity. An interesting and probably challenging open problem would be to bound the error in $p(L)$ given by Th. 1 as a function of the deviation from 2-design as measured by Φ_2 .

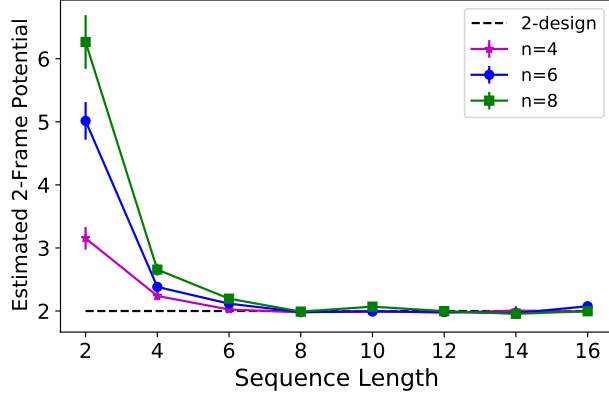


FIG. 1. Plot of Φ_2 defined by Eq. (20) versus sequence length L for $n = 4, 6, 8$. For a 2-design, $\Phi_2 = 2$. Each data point is estimated as the average over 10,000 random unitaries generated by the direct gate set described in Sec. IV.

IV. EXPERIMENT

We implement mirror benchmarking on the Honeywell System Model H1 quantum computer. This system contains 10 trapped-ion qubits in a linear QCCD architecture described in [14, 15]. The native two-qubit gate is the phase-insensitive Mølmer-Sørensen gate [16, 17], given by

$$U_{zz} = e^{-iZZ\pi/4}. \quad (21)$$

A circuit diagram of our implementation is shown in Fig. 2. Each g_i is a circuit layer with a random single-qubit Clifford gate applied to each qubit followed by a native two-qubit gate applied to each qubit pair in a random fully-connected pairing of qubits. Finally, we include Pauli randomization to prevent coherent errors from systematically producing higher survival probabilities. Random Pauli gates that multiply to the identity are inserted between each layer. The second Pauli gate in each product is pushed through the subsequent layer using the commutation relations and combined with the next single-qubit gate.

The results of our experiment are shown in Fig. 3. The figure shows the average $p(L)$ versus $L = 4, 8, 12, 16$ and with qubit number $n = 6, 8, 10$. We only use an even

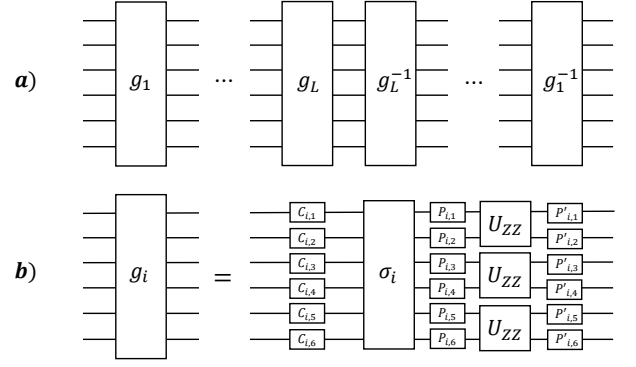


FIG. 2. Mirror benchmarking circuit diagram. **a)** General form for mirror benchmarking with L layers, shown for $n = 6$. **b)** The i -th layer unitary used in our implementation. Random single-qubit Clifford gates $C_{i,j}$ are applied to qubit j . A random permutation $\sigma_i \in S_n$ is applied, and the native U_{zz} gate is then applied to each qubit pair. Random Paulis $P_{i,j}$ are inserted before and pushed through the U_{zz} gates to leave the circuit unitary unchanged. The Paulis $P'_{i,j}$ are combined with the subsequent round of Cliffords before execution on actual hardware.

number of qubits, since increasing to odd $n + 1$ does not increase the number of two-qubit gates in our circuits, which are the leading source of circuit error. For each sequence length, we sample 10 circuits, and repeat each circuit for 100 shots. We insert random Pauli gates before the measurement, so that the constant B can be fixed to $1/2^n$, as described in [18]. The error bars are computed by a bootstrapping procedure adapted from [12]. For each sequence length, the random circuits are resampled with replacement and then a parametric bootstrap is performed on the observed probability distribution for each circuit. The unitarity estimate at $n = 10$ is $u = 0.938(4)$, corresponding to process fidelity bounds of $0.938(4) \leq F(\mathcal{E}) \leq 0.969(2)$ per random fully-connected layer with 5 two-qubit gates.

To study the accuracy and precision of the unitarity estimate, we simulate 100 different mirror benchmarking experiments for $n = 6, 8, 10$ with depolarizing error on the two-qubit gates. For each simulated experiment, the depolarizing parameter was chosen uniformly at random between 0.0 and 1.0×10^{-2} . Figure 4 shows a scatter plot of the estimated unitarity versus depolarizing parameter, with the true unitarity plotted for comparison. The true unitarity for circuit layers consisting of $n/2$ two-qubit gates with uniform depolarizing error is given by a formula that we derive in the appendix. For a single point, the estimation error is the difference between the estimated and true unitarities. The mean of the estimation errors of the simulated data points is less than 2×10^{-4} , and the standard deviations are $1.5, 2.2, 2.6 \times 10^{-3}$ for $n = 6, 8, 10$, respectively. This indicates that for this error model, mirror benchmarking gives an unbiased estimate of the unitarity, to within the numerical precision

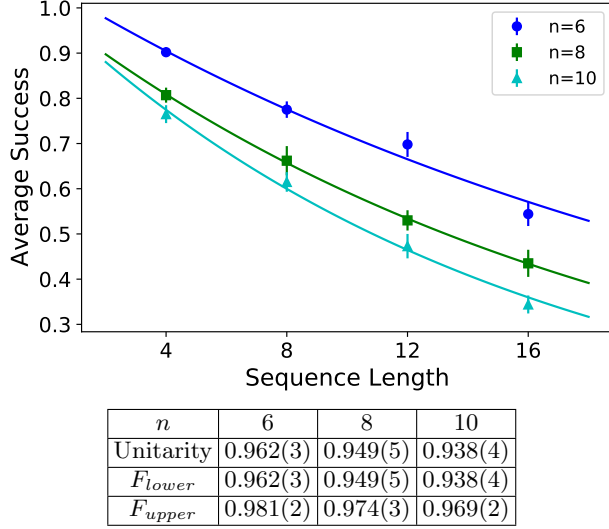


FIG. 3. Mirror benchmarking data plotting $p(L)$ versus L for qubit numbers $n = 6, 8, 10$, with 10 circuits per sequence length, and 100 shots per circuit. The data was taken on the Honeywell System Model H1. The table gives the unitarity estimate obtained by best-fitting to $p(L) = Au^{L-1} + 1/2^n$, as well as the lower and upper bounds on the process fidelity given by Eq. (19).

of the simulation.

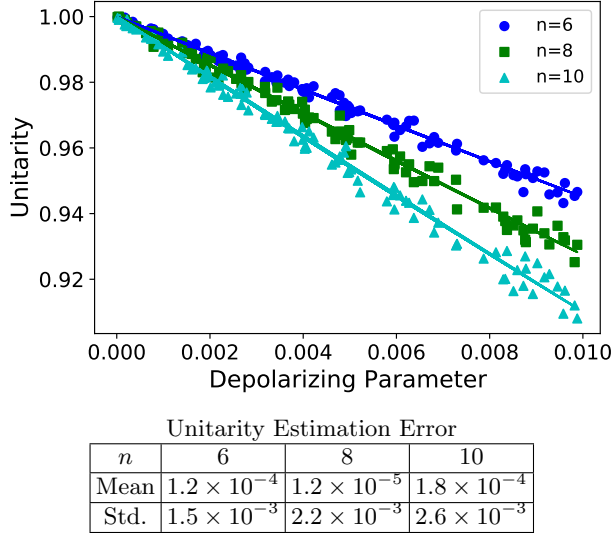


FIG. 4. Scatter plot of unitarity estimates from 100 simulated mirror benchmarking experiments versus two-qubit depolarizing parameter. The solid lines plot the true unitarity. Each experiment used sequence lengths $L = 4, 8, 12, 16$ and 10 circuits per sequence length.

V. DISCUSSION

We have shown that for mirror benchmarking with random circuits, under some assumptions the survival probability decays exponentially according to the unitarity of the average error channel per layer. This justifies the use of mirror benchmarking as a system-level test of quantum computer performance and leads to a number of applications. It is well known that coherent errors can cause large quantum circuits to perform worse than would be predicted from the fidelities of single and two-qubits gates alone [19]. A mirror benchmarking experiment could be performed with and without the use of randomized compiling. If the noise is partially coherent, then the survival probability and extracted unitarity will be higher without randomized compiling, indicating that randomized compiling should be used for real quantum circuits of interest. Apart from providing a system-level benchmark, mirror benchmarking also reduces to a protocol for estimating the unitarity of gate errors, when performed on just one or two qubits. This is an alternative to the protocol in [9], which relies on repeating circuits over multiple measurement settings. We leave an exploration of the ability for mirror benchmarking to diagnose coherent errors to a future work.

We conclude by pointing out some limitations of our present work and open problems. First, we proved our main result under the uniform noise assumption, that is, that \mathcal{E} is the same error channel for every layer g_i . This assumption is unrealistic but is commonly made in the research on RB, and often works well in practice. We speculate that this assumption can be relaxed, as was shown for RB in [20]. Also, we do not present a statistical analysis for the unitarity estimate (i.e. a confidence interval as a function of sample and circuit complexity) in this work. We believe that methods from [21] and [18] can be adapted to our setting, but this is an open problem. Finally, we remark that the layer unitaries in mirror benchmarking in general can be chosen to be whatever one wants. In particular, one could choose Haar random elements of $SU(4)$ for each qubit pair to define a mirrored version of the quantum volume (QV) test [1]. This would solve the problem that QV requires classical simulation and is therefore fundamentally unscalable. We wonder what the relationship is between the survival probability and the heavy outcome probability in ensembles of mirror benchmarking and QV circuits, respectively, and whether mirror benchmarking can be used to extrapolate QV beyond the regime of classical simulatability.

ACKNOWLEDGMENTS

We acknowledge Timothy Proctor for a helpful discussion. We thank Charlie Baldwin and David Hayes and for comments and suggestions. We thank the entire experimental team at Honeywell Quantum Solutions for making this work possible.

-
- [1] A. W. Cross, L. S. Bishop, S. Sheldon, P. D. Nation, and J. M. Gambetta, Validating quantum computers using randomized model circuits, *Phys. Rev. A* **100**, 032328 (2019).
- [2] K. Wright, K. M. Beck, S. Debnath, J. M. Amini, Y. Nam, N. Grzesiak, J.-S. Chen, N. C. Piseni, M. Chmielewski, C. Collins, K. M. Hudek, J. Mizrahi, J. D. Wong-Campos, S. Allen, J. Apisdorf, P. Solomon, M. Williams, A. M. DuCore, A. Blinov, S. M. Kreike-meier, V. Chaplin, M. Keesan, C. Monroe, and J. Kim, Benchmarking an 11-qubit quantum computer, *Nature Communications* **10**, 5464 (2019).
- [3] E. Knill, D. Leibfried, R. Reichle, J. Britton, R. B. Blakestad, J. D. Jost, C. Langer, R. Ozeri, S. Seidelin, and D. J. Wineland, Randomized benchmarking of quantum gates, *Phys. Rev. A* **77**, 012307 (2008).
- [4] E. Magesan, J. M. Gambetta, and J. Emerson, Scalable and robust randomized benchmarking of quantum processes, *Phys. Rev. Lett.* **106**, 180504 (2011).
- [5] T. J. Proctor, A. Carignan-Dugas, K. Rudinger, E. Nielsen, R. Blume-Kohout, and K. Young, Direct randomized benchmarking for multiqubit devices, *Phys. Rev. Lett.* **123**, 030503 (2019).
- [6] R. Blume-Kohout and K. C. Young, A volumetric framework for quantum computer benchmarks, *Quantum* **4**, <https://doi.org/10.22331/q-2020-11-15-362> (2020).
- [7] T. Proctor, K. Rudinger, K. Young, E. Nielsen, and R. Blume-Kohout, Measuring the capabilities of quantum computers (2020), arXiv:2008.11294 [quant-ph].
- [8] J. J. Wallman and J. Emerson, Noise tailoring for scalable quantum computation via randomized compiling, *Phys. Rev. A* **94**, 052325 (2016).
- [9] J. Wallman, C. Granade, R. Harper, and S. T. Flammia, Estimating the coherence of noise, *New Journal of Physics* **17**, 113020 (2015).
- [10] C. Dankert, R. Cleve, J. Emerson, and E. Livine, Exact and approximate unitary 2-designs and their application to fidelity estimation, *Phys. Rev. A* **80**, 012304 (2009).
- [11] M. A. Nielsen, A simple formula for the average gate fidelity of a quantum dynamical operation, *Physics Letters A* **303**, 249 (2002).
- [12] A. Meier, *Randomized Benchmarking of Clifford Operators*, Ph.D. thesis, University of Colorado Boulder (2013).
- [13] H. Zhu, Multiqubit clifford groups are unitary 3-designs, *Phys. Rev. A* **96**, 062336 (2017).
- [14] J. M. Pino, J. M. Dreiling, C. Figgatt, J. P. Gaebler, S. A. Moses, M. S. Allman, C. H. Baldwin, M. Foss-Feig, D. Hayes, K. Mayer, C. Ryan-Anderson, and B. Neyenhuis, Demonstration of the trapped-ion quantum ccd computer architecture, *Nature* **592**, 209 (2021).
- [15] R. I. Tobey, K. W. Lee, A. M. Hankin, D. N. Gresh, D. J. Francois, J. G. Bohnet, D. Hayes, and M. J. Bohn, A high-power, low-noise, ultraviolet laser system for trapped-ion quantum computing, in *Conference on Lasers and Electro-Optics* (Optical Society of America, 2020) p. AF3K.3.
- [16] A. Sørensen and K. Mølmer, Entanglement and quantum computation with ions in thermal motion, *Phys. Rev. A* **62**, 022311 (2000).
- [17] P. J. Lee, K.-A. Brickman, L. Deslauriers, P. C. Haljan, L.-M. Duan, and C. Monroe, Phase control of trapped

ion quantum gates, *Journal of Optics B: Quantum and Semiclassical Optics* **7**, S371–S383 (2005).

- [18] R. Harper, I. Hincks, C. Ferrie, S. T. Flammia, and J. J. Wallman, Statistical analysis of randomized benchmarking, *Phys. Rev. A* **99**, 052350 (2019).
- [19] R. Kueng, D. M. Long, A. C. Doherty, and S. T. Flammia, Comparing experiments to the fault-tolerance threshold, *Phys. Rev. Lett.* **117**, 170502 (2016).
- [20] J. J. Wallman, Randomized benchmarking with gate-dependent noise, *Quantum* **2**, 47 (2018).
- [21] J. J. Wallman and S. T. Flammia, Randomized benchmarking with confidence, *New Journal of Physics* **16**, 103032 (2014).

Appendix A: Non-unital error channels

In Sec. II, we assumed that \mathcal{E} is unital, but we can relax this assumption and recover the result of Th. 1 as follows. As a CPTP map, \mathcal{E} can be written as $\mathcal{E} = \Pi_1 + \mathcal{E}_n + \mathcal{E}_u$, where $\mathcal{E}_n = \Pi_2 \mathcal{E} \Pi_1$ and $\mathcal{E}_u = \Pi_2 \mathcal{E} \Pi_2$ are the non-unital and unital parts of \mathcal{E} , respectively. If \mathcal{E} has a non-unital part, then \mathcal{E}^\dagger is not TP. In this case, we make the assumption that the error channel following each inverse layer g_i^{-1} is given by $\mathcal{E}' := \Pi_1 + \mathcal{E}_n + \mathcal{E}_u^\dagger$. That is, the error channel has the same non-unital part but has a unital part that is dual to the unital part of \mathcal{E} . The motivation for this assumption is that we expect control errors on gates (such as over-rotations) to be inverse to the control errors on the corresponding inverse gates. Non-unital errors (such as amplitude damping channels), however, are expected to be constant between the front half and back half of the mirrored circuit. By replacing \mathcal{E}^\dagger with \mathcal{E}' in Sec. II we recover Th. 1.

Appendix B: Bounds on process fidelity from unitary

Let $\mathcal{E}_{ij} = \frac{1}{d} \text{Tr}(P_i \mathcal{E}(P_j))$ be the matrix elements of the error channel in the Pauli basis of the superoperator representation, with the convention that $P_0 = I$. The unitarity is given by

$$u = \frac{1}{D} \sum_{i,j>0} \mathcal{E}_{ij}^2 \geq \frac{1}{D} \sum_{i>0} \mathcal{E}_{ii}^2. \quad (\text{B1})$$

The latter inequality is saturated when \mathcal{E} is a stochastic Pauli channel. Meanwhile, the process fidelity is

$$F(\mathcal{E}) = \frac{1}{d^2} \left(1 + \sum_{i>0} \mathcal{E}_{ii} \right). \quad (\text{B2})$$

From the previous two equations, upper and lower bounds on $F(\mathcal{E})$ for stochastic Pauli channels can be obtained. On one hand, since each $\mathcal{E}_{ii} \in [0, 1]$,

$$\sum_{i>0} \mathcal{E}_{ii}^2 \leq \sum_{i>0} \mathcal{E}_{ii}. \quad (\text{B3})$$

On the other hand, minimizing $\sum_{i>0} \mathcal{E}_{ii}^2$ under the constraint that $\sum_{i>0} \mathcal{E}_{ii} = c$ gives $\mathcal{E}_{ii} = c/D$ for all i , at which point $\sum_{i>0} \mathcal{E}_{ii}^2 = c^2/D$. Therefore,

$$\frac{1}{D} \left(\sum_{i>0} \mathcal{E}_{ii} \right)^2 \leq \sum_{i>0} \mathcal{E}_{ii}^2. \quad (\text{B4})$$

Using these two inequalities and substituting the expressions for u and $F(\mathcal{E})$, after a little algebra we obtain

$$\frac{1}{d^2} (1 + Du) \leq F(\mathcal{E}) \leq \frac{1}{d^2} (1 + D\sqrt{u}). \quad (\text{B5})$$

Appendix C: Unitarity of tensor-product of depolarizing channels

We derive a formula for the unitarity of $n/2$ parallel two-qubit depolarizing channels, with n even. For a

system of dimension d , a depolarizing channel with parameter p acts on a linear operator X as

$$\mathcal{D}(X) = (1 - p)X + p \text{Tr}(X)I/d. \quad (\text{C1})$$

Now fix $d = 4$, corresponding to a two-qubit system, and let $N = n/2$. We are interested in the tensor product channel $\mathcal{D}^{\otimes N}$. For n -qubit Pauli operator $P = P_1 P_2 \cdots P_N$, where P_i is a two-qubit Pauli operator acting on the i -th qubit pair, we have

$$\begin{aligned} \mathcal{D}^{\otimes N}(P_1 \cdots P_N) &= \bigotimes_{i=1}^N \left((1 - p)P_i + \frac{p}{4} \text{Tr}(P_i)I \right) \\ &= \left((1 - p)^N + (1 - p)^{N-1}p \sum_i \delta_{P_i, I} + (1 - p)^{N-2}p^2 \sum_{i < j} \delta_{P_i, I} \delta_{P_j, I} + \dots \right) P_1 \cdots P_N \\ &= \left(\sum_{j=0}^{N-w(P)} \binom{N-w(P)}{j} (1 - p)^{N-j} p^j \right) P_1 \cdots P_N, \end{aligned} \quad (\text{C2})$$

where in the second line we used $\text{Tr}(P_i) = 4\delta_{P_i, I}$, and where $w(P) = |\{i : P_i \neq I\}|$ is the weight of P with respect to the N two-qubit subsystems. The unitarity is given by

$$u(\mathcal{D}^{\otimes N}) = \frac{1}{(4^N - 1)4^N} \sum_{P \neq I} \text{Tr}(P \mathcal{D}^{\otimes N}(P))^2. \quad (\text{C3})$$

We compute the sum over P by first summing over the weights of P . For a given w , there are $15^w \binom{N}{w}$ Paulis of weight w , since there are $\binom{N}{w}$ choices of w subsystems, and $(4^2 - 1) = 15$ different Paulis per subsystem satisfying $P_i \neq I$. Therefore,

$$u(\mathcal{D}^{\otimes N}) = \frac{1}{4^N - 1} \sum_{w=1}^N 15^w \binom{N}{w} \left(\sum_{j=0}^{N-w} \binom{N-w}{j} (1 - p)^{N-j} p^j \right)^2. \quad (\text{C4})$$

This is the equation for the true unitarity that is plotted in Fig. 4.